BIOCHEMISTRY
including biophysical chemistry & molecular biology

Accelerated Publication

pubs.acs.org/biochemistry

# Conformational Selection Is a Dominant Mechanism of Ligand Binding

Austin D. Vogt and Enrico Di Cera*

Edward A. Doisy Department of Biochemistry and Molecular Biology, Saint Louis University School of Medicine, St. Louis, Missouri 63104, United States

**ABSTRACT:** Molecular recognition in biological macromolecules is achieved by binding interactions coupled to conformational transitions that precede or follow the binding step, two limiting mechanisms known as conformational selection and induced fit, respectively. Sorting out the contribution of these mechanisms to any binding interaction remains a challenging task of general interest in biochemistry. Here we show that conformational selection is associated with a vast repertoire of kinetic behaviors, can never be disproved *a priori* as a mechanism of ligand binding, and is sufficient to explain the relaxation kinetics documented experimentally for a large number of systems. On the other hand, induced fit features a narrow spectrum of kinetic behaviors and can be disproved in many cases in which conformational selection offers the only possible explanation. This conclusion offers a paradigm shift in the analysis of relaxation kinetics, with conformational selection acquiring preeminence as a mechanism of ligand binding. The dominant role of conformational selection supports the emerging structural view of the macromolecule as a conformational ensemble from which the ligand selects the initial optimal fit to produce a biological response.

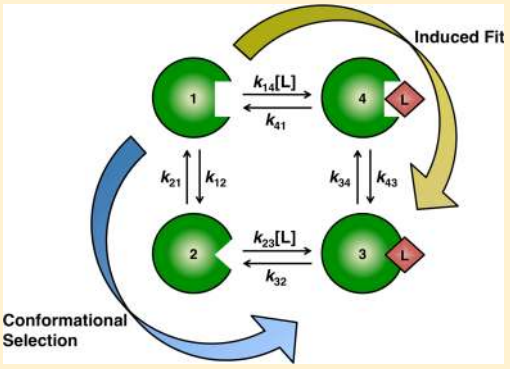


All biological processes proceed through macromolecular interactions that take place over a wide range of time scales and binding affinities. The interaction involves two components: specific binding of the ligand, L, to its macromolecular target, E, and linked conformational changes that precede or follow the binding step. The combination of binding steps and conformational transitions in any given mechanism of recognition generates the repertoire of kinetic behaviors accessible to experimental measurements. The challenge facing the experimentalist is to decipher the nature of conformational transitions involved in the recognition process from analysis of the transient behavior of the system relaxing to equilibrium.[1,2] Once the differential equations associated with the kinetic mechanism are defined, the time evolution of the concentration of each species involved assumes the general form

$$x(t) = A_0 + \sum_{i=1}^{N} A_i \exp(\lambda_i t) = A_0 + \sum_{i=1}^{N} A_i \exp(-k_{\mathrm{obs},i} t) \quad (1)$$

where the $\lambda$ values are the $N$ non-zero eigenvalues of the matrix of the set of differential equations and the $A$ values are the corresponding eigenvectors.[1−3] Each $\lambda$ defines a value of $k_{obs}$ for the relaxation observed experimentally. A system of $N$ independent species gives rise to $N$ independent eigenvalues and relaxations. However, some of the relaxations may be too fast to measure by conventional stopped-flow techniques or may be spectroscopically silent. Analysis of a ligand binding interaction must therefore rely only on the relaxations that can be accessed experimentally, and interpretation of the underlying mechanism should be based on the simplest kinetic scheme consistent with the observations.

Two basic mechanisms of ligand recognition have been widely used in the analysis of relaxation kinetics.[2,4] Both mechanisms envision a conformational isomerization that either precedes or follows the binding step. In the first case (Scheme 1 of Figure 1), originally discussed by Eigen as pre-equilibrium[1,2] and more recently termed conformational selection,[5,6] the macromolecule is assumed to undergo a transition between multiple conformations from which one is selected for binding by the ligand. In this scheme, the number of conformations accessible to the macromolecule decreases upon ligation as the ligand singles out the one with an optimal fit from the preexisting ensemble. In the second case (Scheme 2 of Figure 1), introduced by Koshland as induced fit,[7] the macromolecule is assumed to first bind the ligand and then change its conformation in the bound form to optimize the complex. Here, the number of conformations accessible to the macromolecule increases with ligation. In the case of conformational selection, the macromolecule has a preexisting flexibility to accommodate the ligand. In the case of induced fit, such a feature is unnecessary because the ligand induces the optimal fit with the binding site after the initial complex is formed. When available, structural information about the free and bound forms of the macromolecule is of diagnostic value:

**Received:** July 12, 2013
**Revised:** August 12, 2013
**Published:** August 14, 2013

   dx.doi.org/10.1021/bi400929b | *Biochemistry* 2013, 52, 5723−5729

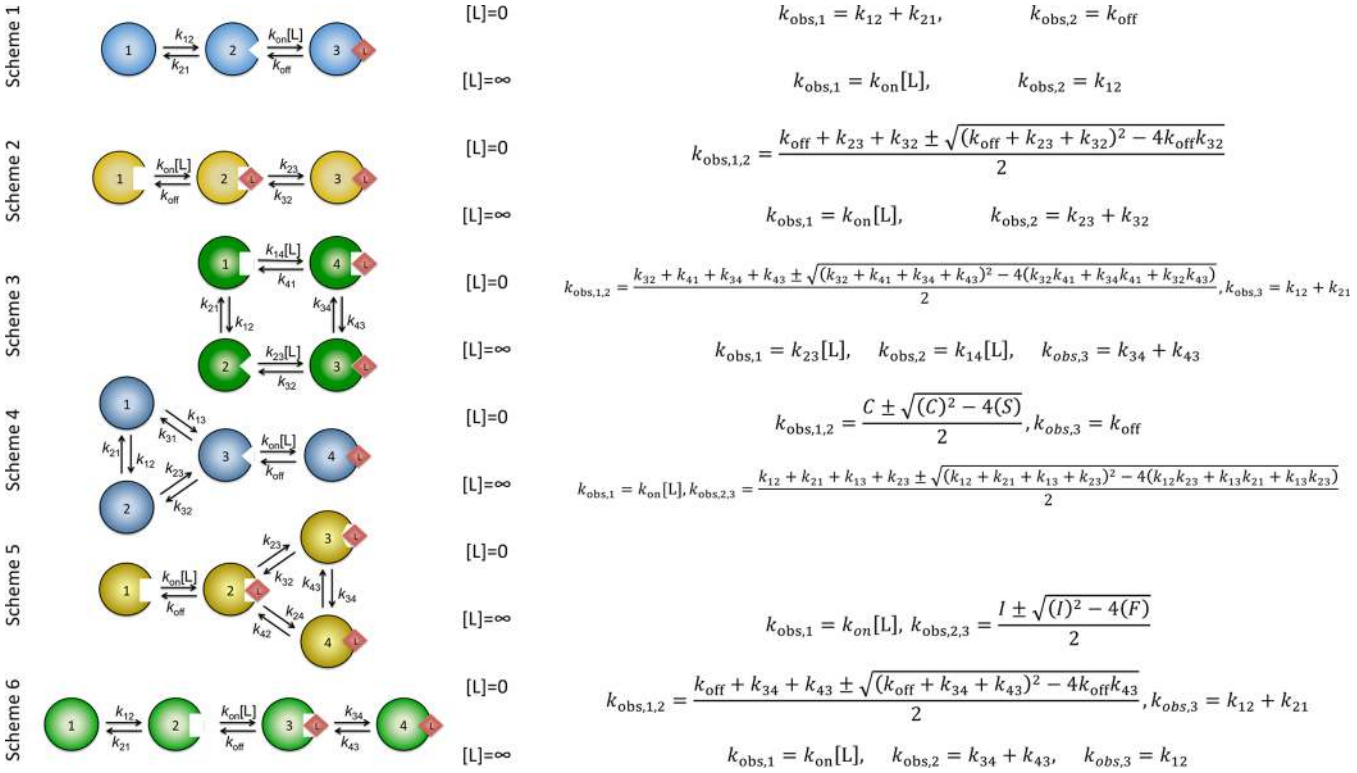


**Figure 1.** Mechanisms of ligand binding discussed in the text with corresponding asymptotic values of $k_{obs}$ in the limits [L] = 0 and [L] = ∞. Schemes 1 and 2 correspond to the well-known conformational selection and induced fit mechanisms of binding, respectively. Scheme 3 is the general linkage scheme, of which Schemes 1 and 2 represent special cases (see also Figure 3). Schemes 4 and 5 represent generalized extensions of Schemes 1 and 2, respectively. Scheme 6 is a special case of Scheme 3, in which the binding interaction with species **1** is negligible. Special notations are as follows: $C = k_{12} + k_{21} + k_{13} + k_{31} + k_{23} + k_{32}$, $S = k_{12}k_{23} + k_{12}k_{31} + k_{12}k_{32} + k_{13}k_{21} + k_{13}k_{23} + k_{13}k_{32} + k_{21}k_{31} + k_{21}k_{32} + k_{23}k_{31}$ (Scheme 4), $I = k_{23} + k_{32} + k_{24} + k_{42} + k_{34} + k_{43}$, and $F = k_{24}k_{32} + k_{23}k_{34} + k_{24}k_{34} + k_{23}k_{42} + k_{32}k_{42} + k_{34}k_{42} + k_{23}k_{43} + k_{24}k_{43} + k_{32}k_{43}$ (Scheme 5).

evidence of multiple conformations in the free form supports conformational selection,[8] and multiple conformations in the bound form support induced fit.[9] When structural information is not available or inconclusive, the distinction between the two mechanisms must be made from the kinetic signatures of ligand binding. Kinetic data are also necessary to derive information about the rate constants governing the recognition process.

The mechanisms in Schemes 1 and 2 (Figure 1) contain three species, of which only two are independent and relax to equilibrium according to two independent exponentials or $k_{obs}$ values that can be derived analytically.[10] The largest $k_{obs}$ is linked to the binding step in both mechanisms and increases asymptotically as $k_{on}[L]$ (Figure 1). The smaller $k_{obs}$ converges to a finite asymptote and conveys information about the conformational transitions. When the smaller $k_{obs}$ is accessible to experimental measurements, the following can be concluded:[10] if $k_{obs}$ decreases with or is independent of [L], then the macromolecule behaves according to conformational selection (Scheme 1 of Figure 1) and induced fit (Scheme 2 of Figure 1) is ruled out unambiguously; if $k_{obs}$ increases with [L], then the macromolecule behaves according to induced fit or conformational selection and neither mechanism is ruled out unambiguously. The latter conclusion refutes the long-held notion that an increase in $k_{obs}$ with [L] is unambiguous proof of induced fit,[2,4,11,12] which is true only when conformational transitions are rate-limiting.[10] The important finding that emerged from the analytical solution of Schemes 1 and 2 in the general case[10] is that conformational selection, unlike induced fit, can never be disproved *a priori* as a mechanism of ligand binding. Indeed, conformational selection is sufficient to account for all possible behaviors of $k_{obs}$ and becomes necessary when $k_{obs}$ decreases with [L].

How rich is the functional repertoire of conformational selection in the general case? When the number of species involved in the kinetic mechanism of ligand binding increases, the analytical solution of the differential equations becomes algebraically intractable. That limits our ability to assess the general validity of conclusions drawn from the analysis of simple kinetic schemes. Here we take an alternative approach and explore the asymptotic behavior of the underlying relaxations for more complex kinetic schemes both analytically and computationally. Conformational selection emerges from this analysis as a dominant mechanism of ligand binding that is sufficient to explain the kinetic behavior of practically all systems reported in the literature thus far.

## METHODS

Simulations were performed using Mathematica (version 8). Values for independent kinetic rate constants were randomly assigned using the RandomVariate function according to $10^{RV}$, where RV is a random number following a normal distribution with $\mu$ = 1.5, 3.0, or 4.5 and $\sigma$ = 0.25, 0.5, 1.5, or 3.0. The overall properties of the various schemes were found to be independent of the values of $\mu$ and $\sigma$ used in the simulations. The results in Figures 4 and 5 refer to $\mu$ = 3 and $\sigma$ = 0.5 to best reproduce experimental data and involved rate constants spanning a range of 5 orders of magnitude. Dependent rate constants due to detailed balancing were defined as follows: $k_{14}$


dx.doi.org/10.1021/bi400929b | *Biochemistry* 2013, 52, 5723−5729

$= (k_{12}k_{23}k_{34}k_{41})/(k_{21}k_{32}k_{43})$, $k_{32} = (k_{31}k_{12}k_{23})/(k_{21}k_{13})$, and $k_{24} = (k_{42}k_{23}k_{34})/(k_{43}k_{32})$ for Schemes 3−5 (Figure 1), respectively. The characteristic equation was solved numerically for each set of randomly assigned rate constants at [L] = 0 and [L] = $10^{51}$, and a total of $10^6$ sets of solutions were generated for each of the twelve combinations of $\mu$ and $\sigma$ values in each mechanism. The $k_{obs}$ values for each limiting case ([L] = 0 and [L] = ∞) were ordered and paired up such that the largest, second largest, and third largest $k_{obs}$ when [L] = 0 were associated with the largest, second largest, and third largest $k_{obs}$, respectively, when [L] = ∞. The logarithm of the ratio of $k_{obs}$ values for [L] = ∞ and [L] = 0 was used to assess the magnitude and direction of change for $k_{obs}$ with an increasing [L]. Simulations revealed that the largest $k_{obs}$ for all schemes increased according to $k_{on}$[L]. For the general linkage scheme (Scheme 3 of Figure 1), the second largest $k_{obs}$ also increased according to $k_{on,2}$[L], where $k_{on,2}$ is the smaller of the two second-order rate constants for ligand association. All remaining $k_{obs}$ values were found to be several orders of magnitude smaller. These observations guided the assumptions used to derive the analytical expressions for $k_{obs}$ in the limit where [L] = ∞. In particular, $k_{obs,1} \gg k_{obs2}$ and $k_{obs,3}$ for Schemes 1, 2, and 4−6 (Figure 1), while $k_{obs,1}$ and $k_{obs,2} \gg k_{obs,3}$ for Scheme 3 (Figure 1). Additionally, when [L] = ∞, only the highest-order [L] terms were considered to be significant. No further assumptions were required to derive the expressions presented in Figure 1.

## RESULTS

Conformational selection (Scheme 1 of Figure 1) and induced fit (Scheme 2 of Figure 1) exhaust the repertoire of two-step kinetic mechanisms linking ligand binding to conformational transitions when a single saturable $k_{obs}$ is measured experimentally. Improved resolution of stopped-flow spectrometers has made it increasingly common to detect two saturable relaxations. In this case, four possible scenarios should be considered when [L] increases: both $k_{obs}$ values increase, both $k_{obs}$ values decrease, the larger $k_{obs}$ increases and the smaller $k_{obs}$ decreases, the larger $k_{obs}$ decreases and the smaller $k_{obs}$ increases. Figure 2 displays these four scenarios as the quadrants of a plot in which the range of smaller $k_{obs}$ values is displayed as a function of the range of larger $k_{obs}$ values. The range is defined as the ratio of the values of $k_{obs}$ when [L] = ∞ and [L] = 0. The points in the plot map experimental data taken from a variety of systems, namely, immunoglobulins IgE[13] and IgG,[14] protein kinase A,[15] DnaC,[16] CheA,[17] histone deacetylase-like amidohydrolase,[18] polymerase X,[19] 3-hydroxybenzoate 6-hydroxylase,[20] 3-chloroacrylic acid dehalogenase,[21] proline utilization A protein,[22] ACTR and CREB-binding protein,[23] G-quadruplex folding,[24] and DnaB.[25] With the exception of binding of DNP-Ser to IgE SPE7,[13] these points fall in all quadrants but the one in the top left corner where the faster saturable relaxation decreases and the slower saturable relaxation increases with [L]. What mechanism explains the behavior of such systems?

The existence of two saturable $k_{obs}$ values requires at least two steps in the kinetic scheme associated with conformational transitions. In their simplest version, both conformational selection (Scheme 1 of Figure 1) and induced fit (Scheme 2 of Figure 1) do not meet this requirement and cannot explain the behavior of the systems in Figure 2. The two mechanisms are special cases of a general linkage scheme (Figure 3 and Scheme 3 of Figure 1) in which the macromolecule is assumed to exist in two alternative conformations each capable of binding the ligand at a single site.[2,11] The equilibrium properties of this scheme are well-known and form the basis of linkage thermodynamics.[26,27] The steady state properties have also been discussed in great detail first by Botts and Morales[28] in connection with the action of a modifier on enzyme activity and then by Hill[3] in the context of energy transduction. Recent discussions about the linkage scheme have been presented in terms of mutational analysis,[29] fluxes,[30] and diffusion-controlled reactions.[31] The four species in the linkage scheme are

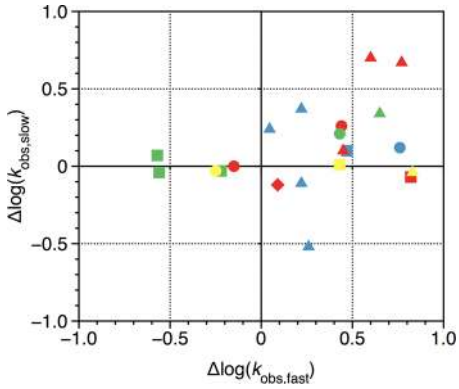


**Figure 2.** Four-quadrant plot with experimental data. The range of the smaller $k_{obs}$ is plotted as a function of the range of the larger $k_{obs}$ for the following experimental systems: IgE (green squares), IgG (green circle), protein kinase A (red circles), DnaC (yellow circle), CheA (yellow triangle), histone deacetylase-like amidohydrolase (blue square), polymerase X (yellow square), 3-hydroxybenzoate 6-hydroxylase (green triangle), 3-chloroacrylic acid dehalogenase (red square), proline utilization A protein (blue circle), ACTR and CREB-binding protein (red diamond), $K^+$-mediated G-quadruplex folding (red triangles), and DnaB (blue triangles). The range is defined as the ratio of the values of $k_{obs}$ for [L] = ∞ and [L] = 0. Multiple points using the same color and shape indicate different ligands binding to the same macromolecule. Points in the top right quadrant indicate that both $k_{obs}$ values increase. Points in the bottom right quadrant indicate a larger $k_{obs}$ that increases coupled to a smaller $k_{obs}$ that decreases. Points in the bottom left quadrant indicate that both $k_{obs}$ values decrease. Points in the top left quadrant indicate a larger $k_{obs}$ that decreases coupled with a smaller $k_{obs}$ that increases, a scenario confined exclusively to binding of DNP-Ser to IgE SPE7.[13]

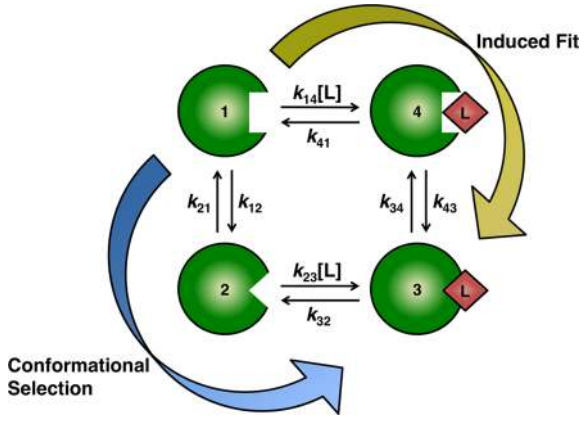


**Figure 3.** General linkage scheme (Scheme 3 of Figure 1) with conformational selection and induced fit as special cases. Species **1** and **2** represent two species with differing affinities for ligand L. Deletion of species **4** yields conformational selection (Scheme 1 of Figure 1), while removal of species **2** produces induced fit (Scheme 2 of Figure 1).


dx.doi.org/10.1021/bi400929b | *Biochemistry* 2013, 52, 5723−5729

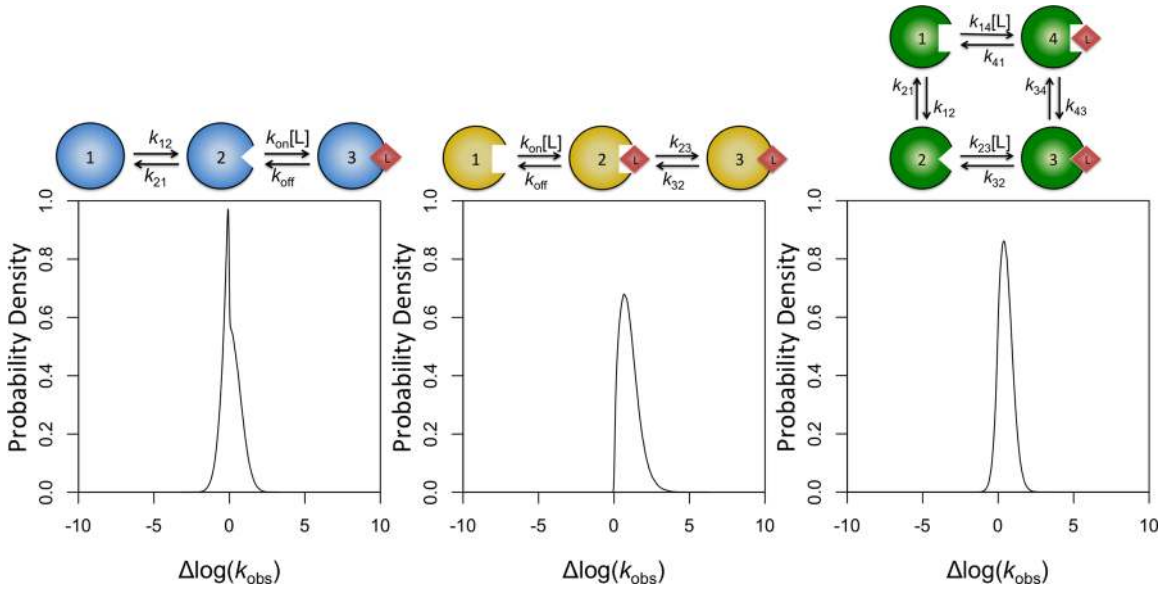


**Figure 4.** Distribution of the range of saturable $k_{obs}$ values, computed as the ratio between the values for [L] = ∞ and [L] = 0, for conformational selection (Scheme 1 of Figure 1), induced fit (Scheme 2 of Figure 1), and the general linkage scheme in Figure 3 (Scheme 3 of Figure 1). Negative values indicate simulations in which $k_{obs}$ decreases with an increasing [L], while positive values indicate simulations in which $k_{obs}$ increases with [L]. Individual rate constants in these simulations varied independently over a range of 5 orders of magnitude.

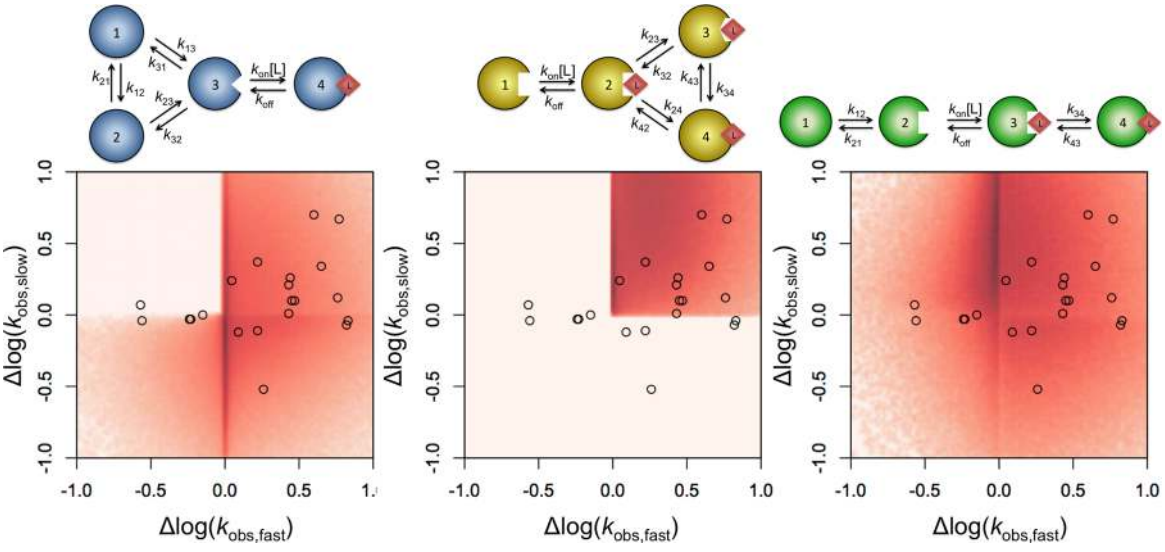


**Figure 5.** Four-quadrant plot with the simulations of extended conformational selection (Scheme 4 of Figure 1), extended induced fit (Scheme 5 of Figure 1), and the mixed scheme (Scheme 6 of Figure 1). Simulations were performed as described in Methods, and the results are plotted in the form of a density map. Experimental data displayed in Figure 2 (○) are overlaid on the simulations for comparison. The best fits of the experimental data to the extended conformational selection and mixed models were obtained by increasing the standard deviation used to generate the rate constants ($\sigma$ = 3.0). Removing the single point of binding of DNP-Ser to IgE SPE7 in the top left quadrant allows Scheme 4 to completely explain the observed experimental distributions shown in Figure 2 ($\chi^2$ = 2.32; $\alpha$ = 5.99). On the other hand, Scheme 6 gives a statistically significant worse fit of the observed distribution ($\chi^2$ = 20.25; $\alpha$ = 7.82).

numbered sequentially to simplify the notation for the kinetic rates. Here, $k_{14}$ ($M^{-1}$ $s^{-1}$) is the second-order association rate constant for binding of ligand to species **1**, and $k_{23}$ ($M^{-1}$ $s^{-1}$) is the second-order association rate constant for binding of ligand to species **2**. Both rate constants are analogous to the $k_{on}$ used in the simpler Schemes 1 and 2 (Figure 1). $k_{41}$ ($s^{-1}$) is the first-order rate constant for dissociation of the complex (species **4**) into species **1**, while $k_{32}$ ($s^{-1}$) is the rate constant for dissociation from species **3** to species **2**. Again, both rate constants are analogous to $k_{off}$ used in the simpler Schemes 1 and 2 (Figure 1). $k_{12}$ ($s^{-1}$) and $k_{21}$ ($s^{-1}$) are the first-order rate constants for conformational isomerization between the free species, and $k_{34}$ ($s^{-1}$) and $k_{43}$ ($s^{-1}$) are the analogous rate constants for isomerization between the bound species. Of the four species in the general linkage scheme, only three are independent and associated with three distinct relaxations or $k_{obs}$. The behavior of the various relaxations for finite [L] is algebraically intractable but easier to discuss in the relevant limits [L] = 0 and [L] = ∞, where the macromolecule is either free or bound to the ligand. When [L] = 0, two of the three relaxations depend on the properties of the bound ensemble [$k_{34}$, $k_{43}$, $k_{41}$, and $k_{32}$ (Figure 1)], while one relaxation equals


dx.doi.org/10.1021/bi400929b | *Biochemistry* 2013, 52, 5723−5729

the sum $k_{12} + k_{21}$, which gives the rate of equilibration between the two possible conformations of the macromolecule in the absence of ligand. The precise ordering of the three $k_{obs}$ values, from largest to smallest, depends on the relative magnitudes of the rate constants. When [L] = ∞, two of the three independent $k_{obs}$ values increase linearly with [L], consistent with the presence of two independent binding steps in the general linkage scheme. The third and smallest $k_{obs}$ plateaus at $k_{34} + k_{43}$, which corresponds to the rate of equilibration between the two possible conformations of the macromolecule in the bound form. Although the scheme has two steps reflecting conformational transitions, it is associated with only one saturable relaxation that may increase or decrease with [L] depending on whether $k_{34} + k_{43}$ is greater or smaller than the value for [L] = 0. The possible range of such $k_{obs}$ values is plotted in Figure 4 for a large number of simulated cases and is reproduced almost entirely by conformational selection.

In addition to being unable to generate two saturable relaxations as required by the experimental data in Figure 2, the general linkage scheme features a kinetic repertoire no richer than that of its special case conformational selection (Figure 4). A kinetic mechanism in which conformational transitions are more numerous than binding steps becomes of interest. Consider the extension of the basic conformational selection scheme to include a third conformation in the free form (Scheme 4 of Figure 1). Of the three relaxations in the scheme, one reflects the binding step and increases linearly with [L] when [L] = ∞, but the other two are saturable and can either increase or decrease with [L] yet never in a combination where the larger decreases when the smaller increases. Remarkably, that matches the distribution of $k_{obs}$ values observed experimentally with the exception of a single case (Figure 5). The population distributions predicted for this scheme depend on the standard deviation used to generate the rate constants in the simulation. As the range of kinetic rate constants increases, the scheme predicts that both $k_{obs}$ values will increase in 49% of the simulations (52% observed experimentally), the larger $k_{obs}$ will increase and the smaller $k_{obs}$ will decrease in 32% of simulations (24% observed experimentally), and both $k_{obs}$ values will decrease in 19% of the simulations (19% observed experimentally). In none of the simulations is a decrease in the larger $k_{obs}$ coupled with an increase in the smallest $k_{obs}$. An analogous extension of the basic induced fit scheme to include a third conformation in the bound form (Scheme 5 of Figure 1) also produces three relaxations. One reflects the binding step and increases linearly with [L] when [L] = ∞, but the other two saturable relaxations always increase with [L] and populate only the top right quadrant of the plot (Figure 5). The inability of induced fit to produce a relaxation that decreases with [L] appears to be a general property that limits application of this mechanism in the analysis of ligand binding data. On the other hand, conformational selection is more versatile and offers a sufficient explanation of the kinetics of ligand binding for a large number of different systems.

It is of interest to explore which kinetic mechanism would produce relaxations that populate the plot in Figure 2 in its entirety. Going back to the general linkage scheme (Figure 3 and Scheme 3 of Figure 1), we note that elimination of one binding step keeps the number of relaxations unchanged but increases the number of saturable $k_{obs}$ values from one to two (Scheme 6 of Figure 1). The transformation produces a linearized scheme with a preexisting equilibrium between two forms, allowing selective binding to one of the forms and subsequent isomerization to a second bound form. The resulting mechanism is a mixture of conformational selection and induced fit, and its properties have been discussed previously under certain approximations.[16,32] It can be shown mathematically that when [L] = 0 two of the relaxations from this mixed scheme (Scheme 6 of Figure 1) are equivalent to the two asymptotic limits of induced fit (Scheme 2 of Figure 1) and depend on the rates of isomerization between the bound conformations ($k_{34}$ and $k_{43}$) and the rate of ligand dissociation ($k_{32}$). The third relaxation is equal to $k_{12} + k_{21}$, i.e., the equilibration rate between the two conformations in the free form. These asymptotes are minimally altered from those of the general linkage scheme (Scheme 3 of Figure 1). In the limit where [L] = ∞, the largest $k_{obs}$ grows as $k_{23}$[L] (nonsaturable relaxation) while the remaining two $k_{obs}$ values plateau at the finite values of $k_{12}$ and $k_{34} + k_{43}$, corresponding to the asymptotes of the saturable relaxations in Schemes 1 and 2, respectively. Linearization of the general linkage scheme generates two saturable relaxations that may either increase or decrease with an increasing [L] independent of each other (Figure 5), thereby covering the entire spectrum of possible kinetic behaviors for two saturable relaxations. In addition, five of the six asymptotic values for the three relaxations contain information about the rates of conformational isomerization (Scheme 6 of Figure 1).

## DISCUSSION

The main conclusion of our analysis is that relaxation kinetics cannot disprove conformational selection as a mechanism of ligand binding when one or two saturable relaxations are accessible to experimental measurements. We would like to propose as a conjecture that this conclusion applies generally to any number of saturable relaxations. Indeed, extension of Scheme 4 (Figure 1) to include four free species produces three saturable $k_{obs}$ values, all of which can either increase or decrease with [L]. The argument that conformational selection is disproved by enzymes with lid-gated active sites such as ribokinase,[33] adenosine kinase,[34] and glucokinase,[9] where the conformational change may only follow the binding step,[35] is easily refuted. The closed conformation of the enzyme may preexist in the absence of ligand, no matter how energetically unfavorable, making the mixed scheme (Scheme 6 of Figure 1) ideally suited to describing the relaxation properties of such enzymes.

The preponderance of systems relaxing to equilibrium with a single $k_{obs}$ increasing with [L] to a saturable level has been used for decades as evidence of induced fit as a dominant mechanism of ligand binding.[1,2,4,11,12] We now know that this conclusion is incorrect: conformational selection easily accounts for a $k_{obs}$ that increases with [L] to a saturable level when the value of $k_{off}$ for ligand dissociation is slower than the rates of isomerization of the preexisting conformations of the macromolecule.[10] Furthermore, the number of systems directly disproving induced fit with $k_{obs}$ decreasing with [L] is rapidly expanding and includes alkaline phosphatase,[32] glucokinase,[36] several trypsin-like proteases,[10,12,37−42] immunoglobulin IgE,[43] and DNA in its B to Z transition.[44] The richer repertoire of kinetic behaviors associated with conformational selection is not limited to the case of a single saturable relaxation but extends to the case of two saturable relaxations so abundantly represented in the literature.[13−25] With a single exception, the entire landscape of kinetic properties displayed by these systems (Figure 2) is captured by an extension of conforma-

tional selection to include a third conformation in the ensemble of free forms available to the macromolecule (Figure 5). As the number of preexisting conformations increases, so does the number of saturable relaxations, thereby making conformational selection capable of accounting for even more complex ligand binding kinetics. A paradigm shift in which conformational selection acquires preeminence as a mechanism of ligand binding emerges.

The combination of conformational selection and induced fit produces a mixed scheme (Scheme 6 of Figure 1) whose properties expand those of conformational selection alone and explain the peculiar case of the rate of a fast relaxation decreasing when the rate of a slow relaxation increases (Figure 5). Although this scenario has so far occurred in a single case reported in the literature,[13] its interpretation requires addition of induced fit to the mechanism of ligand binding. The richness of kinetic behaviors associated with conformational selection, either alone (Schemes 1 and 4 of Figure 1) or in combination with induced fit (Scheme 6 of Figure 1), offers functional support to the emerging view of the macromolecule as a conformational ensemble[6,45,46] promoted by NMR[47] and X-ray crystallography.[8] Thermal fluctuations generate a large number of interconverting states compatible with the allowed folds from which the ligand selects the most complementary one(s) for optimal fit. The ensemble view of the macromolecule agrees well with the fact that conformational selection can never be disproved as a mechanism of ligand binding, which supports the conclusion that the preexistence of alternative conformations is a fundamental property of all macromolecules. This conclusion is not incompatible with induced fit providing an additional mechanism for optimization of the complex, and the scenario envisioned by the mixed scheme (Scheme 6 of Figure 1) is likely to become more common as our ability to explore the conformational landscape of the macromolecule improves. Indeed, maltose binding protein shows structural evidence of conformational transitions preceding and following the binding step.[47,48]

## AUTHOR INFORMATION


### Corresponding Author

*Department of Biochemistry and Molecular Biology, Saint Louis University School of Medicine, St. Louis, MO 63104. E-email: enrico@slu.edu. Telephone: (314) 977-9201. Fax: (314) 977-9206.



### Funding

This work was supported in part by National Institutes of Health Grants HL49413, HL73813, HL95315, and HL112303.


### Notes

The authors declare no competing financial interest.

## REFERENCES


(1) Eigen, M. (1957) Determination of general and specific ionic interactions in solution. *Discuss. Faraday Soc. 24*, 25−36.

(2) Eigen, M. (1968) New looks and outlooks in physical enzymology. *Q. Rev. Biophys. 1*, 3−33.

(3) Hill, T. L. (1977) *Free Energy Transduction in Biology*, Academic Press, New York.

(4) Tummino, P. J., and Copeland, R. A. (2008) Residence time of receptor-ligand complexes and its effect on biological function. *Biochemistry 47*, 5481−5492.

(5) Boehr, D. D., Nussinov, R., and Wright, P. E. (2009) The role of dynamic conformational ensembles in biomolecular recognition. *Nat. Chem. Biol. 5*, 789−796.

(6) James, L. C., and Tawfik, D. S. (2003) Conformational diversity and protein evolution: A 60-year-old hypothesis revisited. *Trends Biochem. Sci. 28*, 361−368.

(7) Koshland, D. E. (1958) Application of a Theory of Enzyme Specificity to Protein Synthesis. *Proc. Natl. Acad. Sci. U.S.A. 44*, 98−104.

(8) Pozzi, N., Vogt, A. D., Gohara, D. W., and Di Cera, E. (2012) Conformational selection in trypsin-like proteases. *Curr. Opin. Struct. Biol. 22*, 421−431.

(9) Rivas-Pardo, J. A., Herrera-Morande, A., Castro-Fernandez, V., Fernandez, F. J., Vega, M. C., and Guixe, V. (2013) Crystal Structure, SAXS and Kinetic Mechanism of Hyperthermophilic ADP-Dependent Glucokinase from *Thermococcus litoralis* Reveal a Conserved Mechanism for Catalysis. *PLoS One 8*, e66687.

(10) Vogt, A. D., and Di Cera, E. (2012) Conformational Selection or Induced Fit? A Critical Appraisal of the Kinetic Mechanism. *Biochemistry 51*, 5894−5902.

(11) Halford, S. E. (1972) *Escherichia coli* alkaline phosphatase. Relaxation spectra of ligand binding. *Biochem. J. 126*, 727−738.

(12) Fersht, A. R. (1999) *Enzyme Structure and Mechanism*, Freeman, New York.

(13) James, L. C., and Tawfik, D. S. (2005) Structure and kinetics of a transient antibody binding intermediate reveal a kinetic discrimination mechanism in antigen recognition. *Proc. Natl. Acad. Sci. U.S.A. 102*, 12730−12735.

(14) Foote, J., and Milstein, C. (1994) Conformational isomerism and the diversity of antibodies. *Proc. Natl. Acad. Sci. U.S.A. 91*, 10370−10374.

(15) Ni, Q., Shaffer, J., and Adams, J. A. (2000) Insights into nucleotide binding in protein kinase A using fluorescent adenosine derivatives. *Protein Sci. 9*, 1818−1827.

(16) Galletto, R., Jezewska, M. J., and Bujalowski, W. (2005) Kinetics of Allosteric Conformational Transition of a Macromolecule Prior to Ligand Binding: Analysis of Stopped-Flow Kinetic Experiments. *Cell Biochem. Biophys. 42*, 121−144.

(17) Eaton, A. K., and Stewart, R. C. (2010) Kinetics of ATP and TNP-ATP binding to the active site of CheA from *Thermotoga maritima*. *Biochemistry 49*, 5799−5809.

(18) Sykora, J., and Meyer-Almes, F.-J. (2010) Mechanism of binding of the inhibitor (E)-3-(furan-2-yl)-N-hydroxyacrylamide to a histone deacetylase-like amidohydrolase. *Biochemistry 49*, 1418−1424.

(19) Jezewska, M. J., Szymanski, M. R., and Bujalowski, W. (2011) Kinetic mechanism of the ssDNA recognition by the polymerase X from African Swine Fever Virus. Dynamics and energetics of intermediate formations. *Biophys. Chem. 158*, 9−20.

(20) Sucharitakul, J., Wongnate, T., Montersino, S., van Berkel, W. J. H., and Chaiyen, P. (2012) Reduction kinetics of 3-hydroxybenzoate 6-hydroxylase from *Rhodococcus jostii* RHA1. *Biochemistry 51*, 4309−4321.

(21) Huddleston, J. P., Schroeder, G. K., Johnson, K. A., and Whitman, C. P. (2012) A pre-steady state kinetic analysis of the αY60W mutant of trans-3-chloroacrylic acid dehalogenase: Implications for the mechanism of the wild-type enzyme. *Biochemistry 51*, 9420−9435.

(22) Moxley, M. A., and Becker, D. F. (2012) Rapid reaction kinetics of proline dehydrogenase in the multifunctional proline utilization A protein. *Biochemistry 51*, 511−520.

(23) Dogan, J., Schmidt, T., Mu, X., Engstrom, A., and Jemth, P. (2012) Fast association and slow transitions in the interaction between two intrinsically disordered protein domains. *J. Biol. Chem. 287*, 34316−34324.

(24) Zhang, A. Y. Q., and Balasubramanian, S. (2012) The kinetics and folding pathways of intramolecular G-quadruplex nucleic acids. *J. Am. Chem. Soc. 134*, 19297−19308.

(25) Bujalowski, W., and Jezewska, M. J. (2000) Kinetic mechanism of nucleotide cofactor binding to *Escherichia coli* replicative helicase DnaB protein. Stopped-flow kinetic studies using fluorescent, ribose-, and base-modified nucleotide analogues. *Biochemistry 39*, 2106−2122.

(26) Di Cera, E. (1995) *Thermodynamic Theory of Site-Specific Binding Processes in Biological Macromolecules*, Cambridge University Press, Cambridge, U.K.
(27) Wyman, J., and Gill, S. J. (1990) *Binding and Linkage*, University Science Books, Mill Valley, CA.
(28) Botts, J., and Morales, M. (1953) Analytical description of the effects of modifiers and of multivalency upon the steady state catalyzed reaction rate. *Trans. Faraday Soc. 49*, 696−707.
(29) Weikl, T. R., and von Deuster, C. (2009) Selected-fit versus induced-fit protein binding: Kinetic differences and mutational analysis. *Proteins 75*, 104−110.
(30) Hammes, G. G., Chang, Y. C., and Oas, T. G. (2009) Conformational selection or induced fit: A flux description of reaction mechanism. *Proc. Natl. Acad. Sci. U.S.A. 106*, 13737−13741.
(31) Zhou, H. X. (2010) From induced fit to conformational selection: A continuum of binding mechanism controlled by the timescale of conformational transitions. *Biophys. J. 98*, L15−L17.
(32) Halford, S. E. (1971) *Escherichia coli* alkaline phosphatase. An analysis of transient kinetics. *Biochem. J. 125*, 319−327.
(33) Sigrell, J. A., Cameron, A. D., and Mowbray, S. L. (1999) Induced fit on sugar binding activates ribokinase. *J. Mol. Biol. 290*, 1009−1018.
(34) Reddy, M. C., Palaninathan, S. K., Shetty, N. D., Owen, J. L., Watson, M. D., and Sacchettini, J. C. (2007) High resolution crystal structures of *Mycobacterium tuberculosis* adenosine kinase: Insights into the mechanism and specificity of this novel prokaryotic enzyme. *J. Biol. Chem. 282*, 27334−27342.
(35) Sullivan, S. M., and Holyoak, T. (2008) Enzymes with lid-gated active sites must operate by an induced fit mechanism instead of conformational selection. *Proc. Natl. Acad. Sci. U.S.A. 105*, 13829−13834.
(36) Kim, Y. B., Kalinowski, S. S., and Marcinkeviciene, J. (2007) A pre-steady state analysis of ligand binding to human glucokinase: Evidence for a preexisting equilibrium. *Biochemistry 46*, 1423−1431.
(37) Fersht, A. R., and Requena, Y. (1971) Equilibrium and rate constants for the interconversion of two conformations of α-chymotrypsin. The existence of a catalytically inactive conformation at neutral p H. *J. Mol. Biol. 60*, 279−290.
(38) Bah, A., Garvey, L. C., Ge, J., and Di Cera, E. (2006) Rapid kinetics of $Na^+$ binding to thrombin. *J. Biol. Chem. 281*, 40049−40056.
(39) Lai, M. T., Di Cera, E., and Shafer, J. A. (1997) Kinetic pathway for the slow to fast transition of thrombin. Evidence of linked ligand binding at structurally distinct domains. *J. Biol. Chem. 272*, 30275−30282.
(40) Papaconstantinou, M. E., Gandhi, P. S., Chen, Z., Bah, A., and Di Cera, E. (2008) $Na^+$ binding to meizothrombin desF1. *Cell. Mol. Life Sci. 65*, 3688−3697.
(41) Gombos, L., Kardos, J., Patthy, A., Medveczky, P., Szilagyi, L., Malnasi-Csizmadia, A., and Graf, L. (2008) Probing conformational plasticity of the activation domain of trypsin: The role of glycine hinges. *Biochemistry 47*, 1675−1684.
(42) Vogt, A. D., Bah, A., and Di Cera, E. (2010) Evidence of the E*-E equilibrium from rapid kinetics of $Na^+$ binding to activated protein C and factor Xa. *J. Phys. Chem. B 114*, 16125−16130.
(43) James, L. C., and Tawfik, D. S. (2005) Structure and kinetics of a transient antibody binding intermediate reveal a kinetic discrimination mechanism in antigen recognition. *Proc. Natl. Acad. Sci. U.S.A. 102*, 12730−12735.
(44) Bae, S., Kim, D., Kim, K. K., Kim, Y. G., and Hohng, S. (2011) Intrinsic Z-DNA is stabilized by the conformational selection mechanism of Z-DNA-binding proteins. *J. Am. Chem. Soc. 133*, 668−671.
(45) Boehr, D. D., McElheny, D., Dyson, H. J., and Wright, P. E. (2006) The dynamic energy landscape of dihydrofolate reductase catalysis. *Science 313*, 1638−1642.
(46) Ma, B., Kumar, S., Tsai, C. J., and Nussinov, R. (1999) Folding funnels and binding mechanisms. *Protein Eng. 12*, 713−720.
(47) Tang, C., Schwieters, C. D., and Clore, G. M. (2007) Open-to-closed transition in apo maltose-binding protein observed by paramagnetic NMR. *Nature 449*, 1078−1082.
(48) Bucher, D., Grant, B. J., and McCammon, J. A. (2011) Induced fit or conformational selection? The role of the semi-closed state in the maltose binding protein. *Biochemistry 50*, 10530−10539.